Deglacial rapid sea level rises caused by ice sheet saddle collapses

Lauren J. Gregoire, Antony J. Payne and Paul J. Valdes

School of Geographical Sciences, University of Bristol, UK.

Manuscript accepted in Nature and published in July 2012.

Citation: Gregoire, L.J., Payne, A.J., Valdes, P.J., 2012. Deglacial rapid sea level rises caused by ice-sheet saddle collapses. Nature 487, 219–222. doi: 10.1038/nature11257.

Publised version available at:

http://www.nature.com/nature/journal/v487/n7406/full/nature11257.html

Several meltwater pulses occurred during the last deglaciation (21-7 ka), sometimes causing significant climate change[1,2]. Around 14 ka, Meltwater Pulse 1a (MWP1a), the largest of these events, produced a sea level rise of 14-18 m in 350 years[3]. This great amount of water came from the retreat of ice sheets, but there is currently no consensus on the source or the cause of this rapid sea level rise[4–6]. We present an ice sheet modelling simulation during which the separation of the Laurentide and Cordilleran ice sheets in North America produces a meltwater pulse, which correlates with MWP1a. Another meltwater pulse is produced when the Labrador and Baffin domes around Hudson Bay separate, which could be associated with the '8,200 year' event, the most pronounced abrupt climate event of the past 9,000 years[7]. For both events, the saddle between two ice domes becomes subject to surface melting because of a general surface lowering, caused by climate warming. The melting then rapidly accelerates as the saddle between the two domes continues to lower, producing 9 m of sea level rise in 500 years.

This mechanism of an ice 'saddle collapse' explains MWP1a and the '8,200 year' event and could help us better understand the consequences of these events on climate.

North America has been cited as the most probable source of MWP1a, because the Laurentide ice sheet that was covering Canada retreated significantly at that time[8]. However, despite the evidence of freshening of the North Atlantic at the time of MWP1a[9,10], one study estimated the contribution of the Laurentide ice sheet to MWP1a to be less than 5.3 m based on the chemical composition of seawater near the ice sheet's southern, eastern and northern runoff outlets[4]. Glacio-isostatic adjustment models disagree on the hemispherical origin of MWP1a[5,6] and glaciological evidence from Antarctica is currently insufficient to rule out a potential contribution from East Antarctica. Disagreements in the source and difficulties in estimating the timing and duration of MWP1a make it difficult to link this event with recorded climate changes[11–13] and determine if the large amount of freshwater released into the oceans during this event had a similar climate impact as other ocean freshening events such as Heinrich Event 1[2].

In a series of ice sheets model simulations of the North American deglaciation, we observed two meltwater pulses that can be associated with MWP1a and the '8,200 year event', caused by a common mechanism. We simulated the deglaciation of the North American with the Glimmer-CISM ice sheet model[14] driven offline with a state of the art transient simulation of the last deglaciation. The climate simulation was itself forced with greenhouse gas concentrations, insolation and freshwater fluxes and prescribed ice sheet extent[8] (Figure S1). Although the climate forcing does not simulate the Bølling-Allerød rapid warming event nor the Younger-Dryas cold period (Figure S2), it does reproduce well the range of warming of the last 21,000 years reconstructed from Greenland ice cores. Our ice sheet simulations reproduce well the extent of ice over North America at the Last Glacial Maximum and during the deglaciation compared to the Ice-5G ice sheet reconstructions[15] (Figure 1). This close

match in ice sheet extent is partly due to the set up of our experiment; the ice sheet extent follows that of Ice-5G because our climate forcing is dependent on that reconstruction. Our ice sheet thickness is, however, independent from Ice-5G and consistent with more recent reconstructions (see Supplementary Text). The decoupling between our results and Ice-5G is most evident in the evolution of the modelled ice volume (Figure 1), which diverges from the reconstruction after 15 ka. The mismatch in ice volume is due to a 2,000 years delay in the separation of the Cordilleran and Laurentide ice sheets in our experiments[8]. This delay could be explained by uncertainties in our climate forcing or some missing dynamical processes (see Supplementary Text). Despite the inaccuracy in the chronology of our simulations, the overall change of ice volume and extent and the rate of our deglaciation is consistent with the Ice-5G reconstruction (Figure 1), giving us confidence in the amplitude and causes of the events observed (see Supplementary Text).

A large meltwater pulse is produced in our experiment around 11.6 ka (Figure 2b) with up to 10×10^3 km^3/yr of ice loss (0.3 SV of freshwater), twice the background melting. This meltwater pulse represents 3.8×10^6 km^3 of water discharged over 500 years, producing a global sea level rise of 9 m in 500 years (Figure 2a). This event coincides with the separation of the Cordilleran ice sheet, over the Rocky Mountains in the west of North America, and the Laurentide ice sheet, covering the plains of Canada (Figure 2c). At 11.6 ka, 80 % of the total North American meltwater flux comes from the Cordilleran-Keewatin region (red box in Figure S3). The Cordilleran and the Laurentide ice sheets separate within 400 years of the start of the meltwater pulse. The Cordilleran ice sheet then significantly thins and disappears over the following 600 years.

The modelled separation of the Laurentide and Cordilleran ice sheets, and its associated meltwater pulse, can be correlated to the MWP1a. Radiocarbon and Luminescence dating indicate that the Ice-Free Corridor between the Laurentide and Cordilleran ice sheets opened

sometime between 15.7 ka and 14 ka (13.5 to 12 ^{14}C ka)[8,16], and not at 11.6 ka as in our model. The separation of the two ice sheets in our model coincides with the production of 9 m of sea level rise in 500 years. This corresponds to 50 to 60 % of the amplitude of MWP1a, which occurred between 14.6 ka and 13.8 ka[3,13,17–19]. It is therefore likely that this freshwater pulse, produced in our model by the opening of the corridor between the Laurentide and Cordilleran ice sheet, corresponds to the MWP1a event (see discussion in Supplementary Text). This result is in agreement with North American deglacial chronologies calibrated with sea level data and evolution of ice extent[6], where the North American ice sheet is estimated to have produced 9.4 to 13.2 m of sea level rise between 14.6 and 14.1 ka. Contributions from the background melting of the Eurasian and Antarctic ice sheet could explain the remaining part of the pulse.

The separation of the two ice sheets in our model induces a lowering of the Cordilleran ice sheet (Figure 3), which results in the deglaciation of the Cordilleran ice sheet within 600 years of the separation of the two ice sheets (supplementary materials). Although in reality, the extent of the Cordilleran ice sheet did not significantly reduce until 11.5 ka[8], field evidence reveals an extreme and widespread thinning of the ice sheet before 12.8 ka (11 ^{14}C ka)[20], and sediment cores suggest a high freshwater input to the North Pacific from 14.7 ka to 12.9 ka[21]. Our results therefore suggest that the thinning of the Cordilleran ice sheet could have thus contributed to MWP1a, which is consistent with a reconstruction of ice sheet drainage chronology[22]. In this case meltwater would have been routed not only towards the Arctic Ocean, the Gulf of Mexico and perhaps the St Laurence[1,23,24], but also towards the Pacific Ocean. We estimate that about a third of MWP1a could have been routed toward the Pacific (Figure S3). The potential distribution of meltwater between the North Atlantic, the Arctic and the North Pacific oceans could have potentially dampened the climate impact of MWP1a on the climate[18]. It could also have influence the pattern of sea level rise observed

99 throughout the world. Hence, fingerprinting the pattern of MWP1a sea level rise may need to
100 be revised.
101 The large meltwater pulse observed in our model is caused by a simple mass balance
102 mechanism associated with the separation of the Cordilleran and Laurentide ice sheets. In our
103 model experiment, progressive warming occurs throughout the deglaciation (Figure S2),
104 which slowly elevates the upper altitude at which surface melting occurs and simultaneously
105 produces a general ice surface lowering. When surface melting starts occurring in the saddle
106 between the Cordilleran and Laurentide ice domes, the ablation zone considerably expands
107 (Figure 3). This then triggers a mass-balance elevation feedback[25], which accelerates surface
108 melting as the saddle lowers and reaches warmer altitudes (Figure 3b). Surface melting peaks
109 when the corridor between the two ice domes opens, it then slows downs as a new
110 equilibrium geometry is reached. This meltwater pulse is also produced in simple warming
111 experiments (see Supplementary Text), which confirms that it is a non-linear response of the
112 ice sheet to climate.
113 MWP1a may not be the only event caused by this saddle collapse mechanism. A smaller
114 meltwater pulse is observed in our simulation around 8.8 ka, reaching a maximum flux of 0.2
115 Sv and producing 9 x 10^6 km^3 of freshwater (2.5 m of sea level rise) in 200 years (Figure 4).
116 This freshwater event happens as the three ice domes around Hudson Bay separate (Figure 4).
117 This event coincides with another freshwater event, the '8200 year event', attributed to the
118 sudden discharge of the proglacial Laurentide lakes (Lake Agassiz and Lake Ojibway)[7]. The
119 amount of meltwater released in our model in 200 year is 4 times greater than the estimates of
120 discharge from the two lakes[7] during the 8200 year event and is consistent with the latest
121 estimates of sea level rise associated with this event of 0.8 m to 2.2 m within 130 years[26].
122 Glaciological reconstruction suggest that the Fox dome over Baffin island and the Labrador
123 dome over Quebec were disconnected from 9 ka, but the Labrador dome was still connected

to the Keewatin Dome and the Fox Dome, through an ice dam[8]. It is the collapse of this ice dam that is thought to have produced a sudden discharge of the proglacial lakes via the Hudson Strait[7]. In our model, most of the meltwater pulse is caused by the melting of the saddle between the Keewatin, Labrador and Fox Domes (Figure 4). Our results suggest that the collapse of the saddle, or ice dam, between the Keewatin and Labrador domes produced a meltwater pulse, which contributed to the freshening of the Labrador Sea. Halfway through this meltwater pulse, the opening of channel between the ice domes would have enabled the sudden discharge of the lakes. This could explain the two stages of this cooling event[27], with the 'saddle collapse' pulse responsible for the longer century time scale climate response and the discharge from Lake Aggasiz being the more rapid cooling occurring halfway through the event.

The mechanism of 'saddle collapse' that produced two meltwater pulses in our simulations of the North American deglaciation reveals the role of multi-dome ice sheet geometries in producing large meltwater pulses in the context of a deglaciation. This can be seen as the reversal mechanism to the one described in the growth of ice caps in Scotland[28] where the topography plays an important role in accelerating the growth. Dynamical processes not yet present in our ice sheet model, involving for example subglacial hydrology or ice streams, could have played a role in facilitating the saddle collapse, thus influencing the timing and potentially the duration of the meltwater pulses. However, the amplitude and the triggering of the pulses can be explained by simple mass balance processes. For the first time, we have associated mass balance processes with specific events of rapid sea level rise of the last deglaciation, MWP1a and the '8,200 year event'. The saddle collapse mechanism could also help identify other rapid sea level rise and ocean freshening events. Moreover, understanding the glaciological cause of meltwater pulses can help determine the routing of meltwater, improve the dating of these events and put the events into the context of climate change.

Method Summary

We simulated the deglaciation of the North American with the Glimmer-CISM ice sheet model with shallow ice approximation[14]. We drove the ice sheet model offline with a state of the art transient simulation of the last deglaciation, performed with the FAMOUS climate model[29]. The climate simulation was itself forced with greenhouse gas concentrations, insolation and freshwater fluxes, which varied continuously throughout the simulation, and geographical changes, which were applies every 1,000 years (Figure S1). Because of high computational demand of the climate model and technical challenges, the ice sheet model could not feedback to the climate model. Ice sheet geometry in the climate model was instead prescribed every 1,000 years based on the Ice-5G reconstruction[15] (Figure S1). We smoothed out the climate forcing to remove artificial steps in the temperature and precipitation forcing, caused by the discontinuous change of ice sheets for each interval (Figure S2). We started our simulation of the deglaciation with spun-up LGM North American ice sheet state, built-up through the last glacial-interglacial cycle using the standard climate-index interpolation technique[30]. Ice sheet mass balance was calculated from the monthly temperature and precipitation fields using an annual Positive Degree Day (PDD) scheme. The temperatures were downscaled onto the Glimmer topography, by using a constant lapse rate of 5 °C km^{-1}. Model parameters shown in Table S1 were adjusted to improve the LGM ice volume, the LGM extent and the rate of uplift throughout the deglaciation compare to reconstructions[8,15].

References:

1. Clark, P. U. Freshwater Forcing of Abrupt Climate Change During the Last Glaciation. Science 293, 283–287 (2001).

2. Bond, G. et al. Correlations Between Climate Records from North-Atlantic Sediments and Greenland Ice. Nature 365, 143–147 (1993).

3. Deschamps, P. et al. Ice-sheet collapse and sea-level rise at the Bolling warming 14,600 years ago. Nature 483, 559–564 (2012).

4. Carlson, A. E. Geochemical constraints on the Laurentide Ice Sheet contribution to Meltwater Pulse 1A. Quaternary Science Reviews 28, 1625–1630 (2009).

5. Clark, P. U., Mitrovica, J. X., Milne, G. A. & Tamisiea, M. E. Sea-Level Fingerprinting as a Direct Test for the Source of Global Meltwater Pulse IA. Science 295, 2438–2441 (2002).

6. Tarasov, L., Dyke, A. S., Neal, R. M. & Peltier, W. R. A data-calibrated distribution of deglacial chronologies for the North American ice complex from glaciological modeling. Earth and Planetary Science Letters 315–316, 30–40 (2012).

7. Barber, D. C. et al. Forcing of the cold event of 8,200 years ago by catastrophic drainage of Laurentide lakes. Nature 400, 344–348 (1999).

8. Dyke, A. S. An outline of North American deglaciation with emphasis on central and northern Canada. Quaternary Glaciations-Extent and Chronology - Part II: North America Volume 2, Part 2, 373–424 (2004).

9. Thornalley, D. J. R., McCave, I. N. & Elderfield, H. Freshwater input and abrupt deglacial climate change in the North Atlantic. Paleoceanography 25, 16 PP. (2010).

10. Aharon, P. Entrainment of meltwaters in hyperpycnal flows during deglaciation superfloods in the Gulf of Mexico. Earth and Planetary Science Letters 241, 260–270 (2006).

11. Stanford, J. D. et al. Timing of meltwater pulse 1a and climate responses to meltwater injections. Paleoceanography 21, 9 PP. (2006).

12. Menviel, L., Timmermann, A., Timm, O. E. & Mouchet, A. Deconstructing the Last Glacial termination: the role of millennial and orbital-scale forcings. Quaternary Science Reviews 30, 1155–1172 (2011).

198 13. Weaver, A. J., Saenko, O. A., Clark, P. U. & Mitrovica, J. X. Meltwater Pulse 1A from
199 Antarctica as a Trigger of the Bølling-Allerød Warm Interval. Science 299, 1709 –1713
200 (2003).
201 14. Rutt, I. C., Hagdorn, M., Hulton, N. R. J. & Payne, A. J. The Glimmer community ice
202 sheet model. J. Geophys. Res. 114, (2009).
203 15. Peltier, W. R. Global glacial isostasy and the surface of the ice-age earth: The ice-5G
204 (VM2) model and grace. Annual Review of Earth and Planetary Sciences 32, 111–149
205 (2004).
206 16. Munyikwa, K., Feathers, J. K., Rittenour, T. M. & Shrimpton, H. K. Constraining the
207 Late Wisconsinan retreat of the Laurentide ice sheet from western Canada using
208 luminescence ages from postglacial aeolian dunes. Quaternary Geochronology 6, 407–422
209 (2011).
210 17. Hanebuth, T., Stattegger, K. & Grootes, P. M. Rapid Flooding of the Sunda Shelf: A
211 Late-Glacial Sea-Level Record. Science 288, 1033–1035 (2000).
212 18. Stanford, J. D. et al. Sea-level probability for the last deglaciation: A statistical analysis of
213 far-field records. Global and Planetary Change 79, 193–203 (2011).
214 19. Bard, E., Hamelin, B. & Fairbanks, R. G. U-Th ages obtained by mass spectrometry in
215 corals from Barbados: sea level during the past 130,000 years. Nature 346, 456–458 (1990).
216 20. Fulton, R. J., Ryder, J. M. & Tsang, S. The Quaternary glacial record of British
217 Columbia, Canada. Quaternary Glaciations-Extent and Chronology - Part II: North America
218 Volume 2, Part 2, 39–50 (2004).
219 21. Davies, M. H. et al. The deglacial transition on the southeastern Alaska Margin:
220 Meltwater input, sea level rise, marine productivity, and sedimentary anoxia.
221 Paleoceanography 26, 18 PP. (2011).

22. Tarasov, L. & Peltier, W. R. A calibrated deglacial drainage chronology for the North American continent: evidence of an Arctic trigger for the Younger Dryas. Quaternary Science Reviews 25, 659–688 (2006).

23. Teller, J. T., Leverington, D. W. & Mann, J. D. Freshwater outbursts to the oceans from glacial Lake Agassiz and their role in climate change during the last deglaciation. Quaternary Science Reviews 21, 879–887 (2002).

24. Murton, J. B., Bateman, M. D., Dallimore, S. R., Teller, J. T. & Yang, Z. Identification of Younger Dryas outburst flood path from Lake Agassiz to the Arctic Ocean. Nature 464, 740–743 (2010).

25. Weertman, J. Stability of Ice-Age Ice Sheets. J. Geophys. Res. 66, PP. 3783–3792 (1961).

26. Li, Y.-X., Törnqvist, T. E., Nevitt, J. M. & Kohl, B. Synchronizing a sea-level jump, final Lake Agassiz drainage, and abrupt cooling 8200 years ago. Earth and Planetary Science Letters 315–316, 41–50 (2012).

27. Rohling, E. J. & Palike, H. Centennial-scale climate cooling with a sudden cold event around 8,200 years ago. Nature 434, 975–979 (2005).

28. Payne, A. & Sugden, D. Topography and ice sheet growth. Earth Surf. Process. Landforms 15, 625–639 (1990).

29. Smith, R. S., Gregory, J. M. & Osprey, A. A description of the FAMOUS (version XDBUA) climate model and control run. Geosci. Model Dev. 1, 53–68 (2008).

30. Gregoire, L. Modelling the Northern Hemisphere Climate and Ice Sheets during the Last Deglaciation. PhD thesis, University of Bristol, Bristol. (2010).

Supplementary Information is linked to the online version of the paper at www.nature.com/nature.

Acknowledgements This work was supported by the Marie Curie Research Training Network NICE (MRTN-CT-2006-036127) and the NERC QUEST (NE/D001846/1) and ORMEN (NE/C509558/1) projects. Glimmer was developed within the NERC National Centre for Earth Observation. We thank Ron Kahana for providing part of the input climate data and for comments on the manuscript. We also thank members of the BRIDGE group and the NICE network for discussions and suggestions. The numerical simulations were carried out using the computational facilities of the BRIDGE group and those of the Advanced Computing Research Centre, University of Bristol - http://www.bris.ac.uk/acrc/.

Author Contributions LJG performed the experiments, the analysis and wrote the manuscript. PJV provided the input climate. All authors contributed to designing the experiments, discussed the results and implications and commented on the manuscript at all stages.

Author information Reprints and permissions information is available at www.nature.com/reprints. The authors declare that they have no competing financial interests. Correspondence and requests for materials should be addressed to LJG (lauren.gregoire@bristol.ac.uk).

Figure

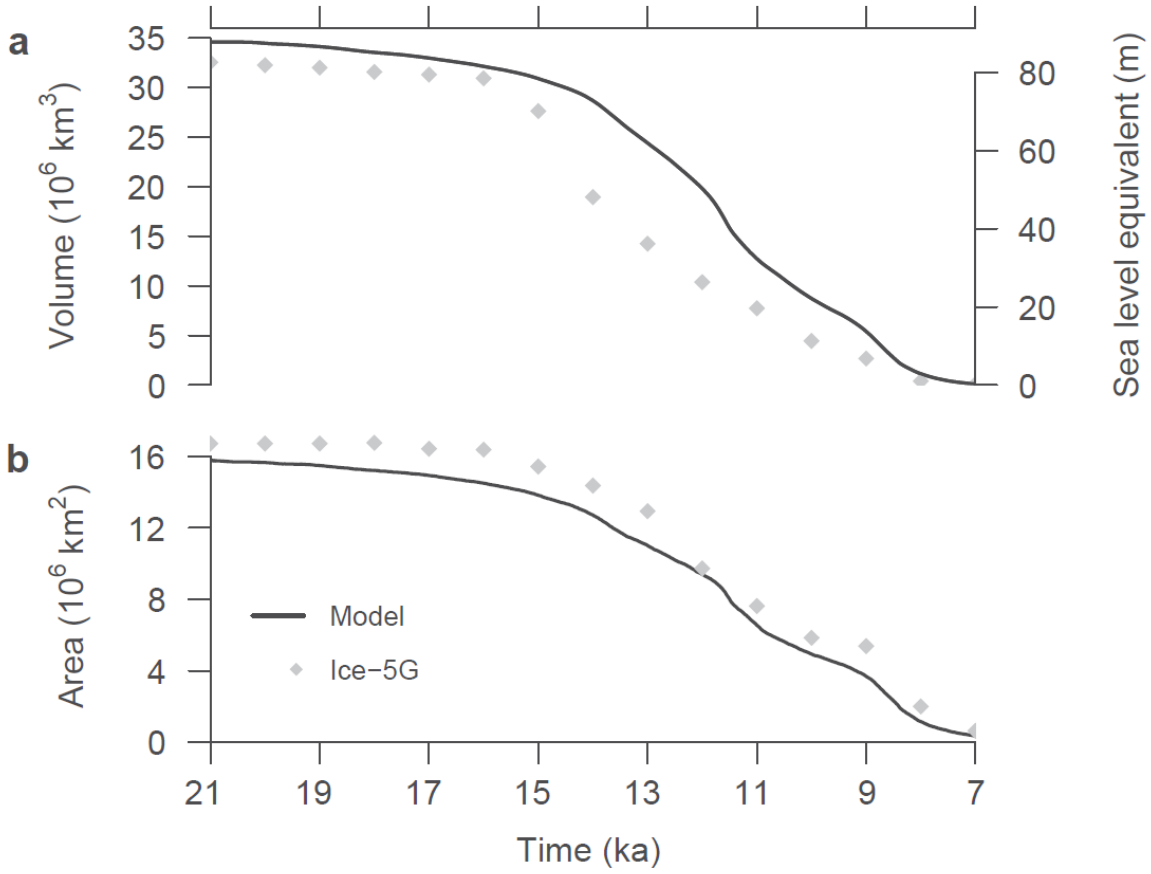

Figure 1: The deglaciation of North America. Evolution of ice volume **a** and area **b** of the North American ice sheet from 21 ka to 7 ka in our model (solid black line) compared to the Ice-5G reconstruction[15](grey diamonds). The delay in our modelled deglaciation could be due to missing dynamical processes or uncertainties in the climate forcing.

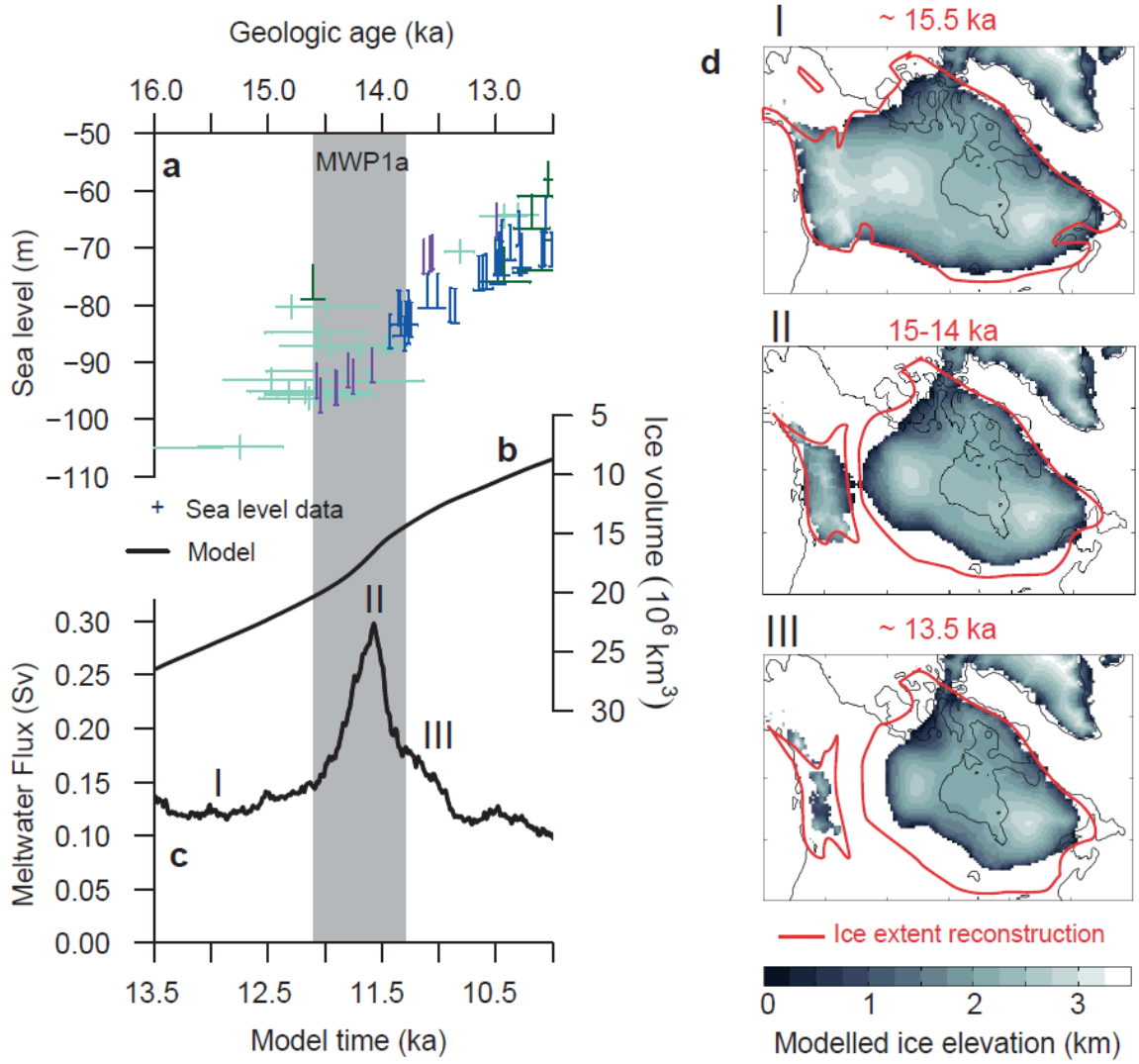

Figure 2: MWP1a in model and data. a, Relative sea level data from the Sunda Shelf (light blue), New Guinea (green), Tahiti (blue) and Barbados (purple). Vertical error bars show the typical depth uncertainty ranges of ±2 m for Sunda Shelf data and +6 m for other data (corals) [11]. Horizontal error bars denote ±1 s.e.m. around the mean age [11]. The vertical grey band denotes the range in MWP1a timing[13,17–19]. Modelled ice volume **b** and meltwater flux **c** (0.1 Sv = 3.2x10^3 km^3/yr of water= 0.8 m/century of sea level rise). **d,** Modelled ice sheet elevation, before (**I**), during (**II**) and after (**III**) the pulse as labelled in **c**, and ice sheet extent reconstruction [8] before, during and after the Ice-Free Corridor opening, with corresponding dates in red. The pulse happens in our model when the corridor between the Laurentide and

Cordilleran ice sheets opens. The opening of this corridor happened between 15 and 14 ka[8,16], which corresponds to the time of MWP1a.

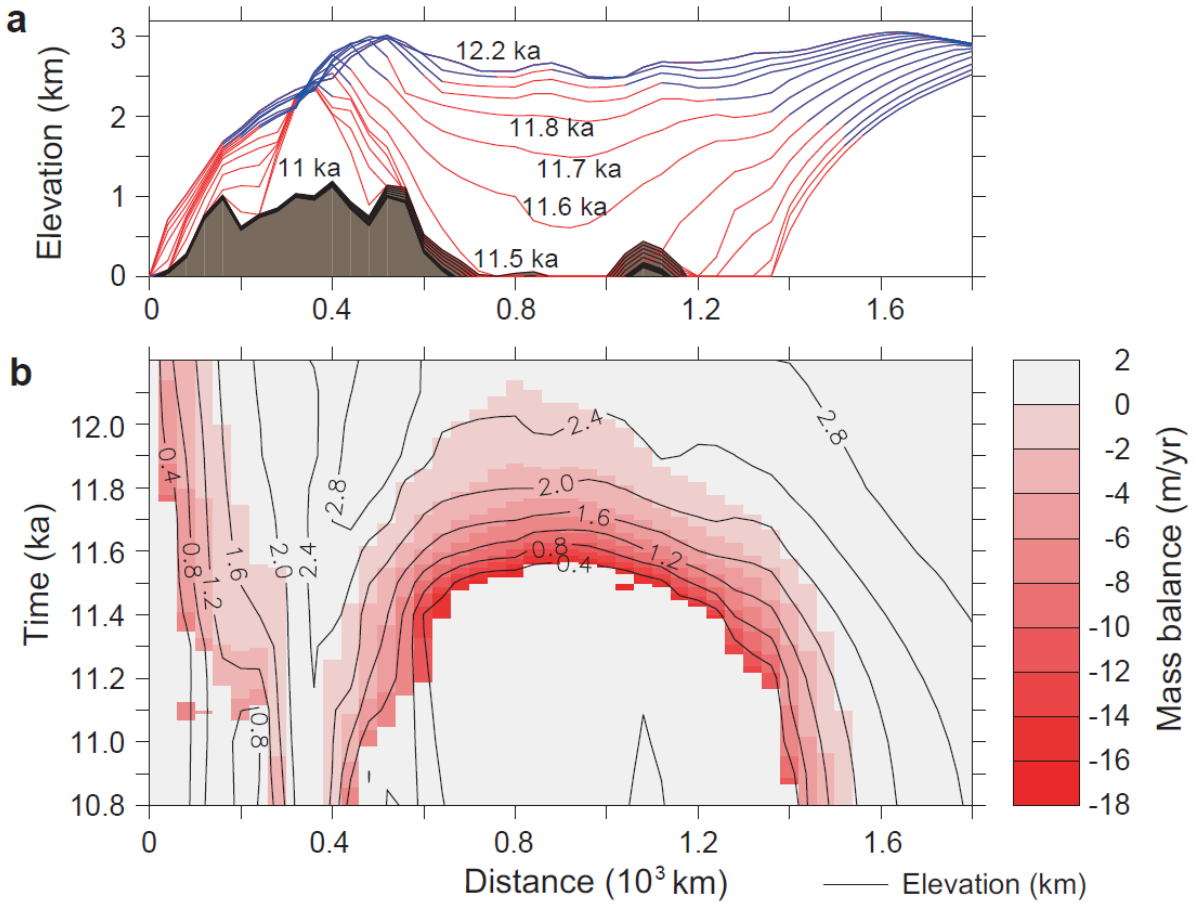

Figure 3: Mechanism of Saddle Collapse. a, Ice sheet elevation (lines) and topography (shaded area) on the cross section (shown in Figure S4) at 100 years interval during the separation of the Cordilleran and Laurentide ice sheet between 12.1 ka and 11 ka in model time. Red lines indicate surface ablation (negative mass balance) and blue lines area of surface accumulation. **b,** Surface mass balance through time along the cross section in shades of red with contours of ice elevation superimposed showing that the mass balance increases primarily because of surface lowering.

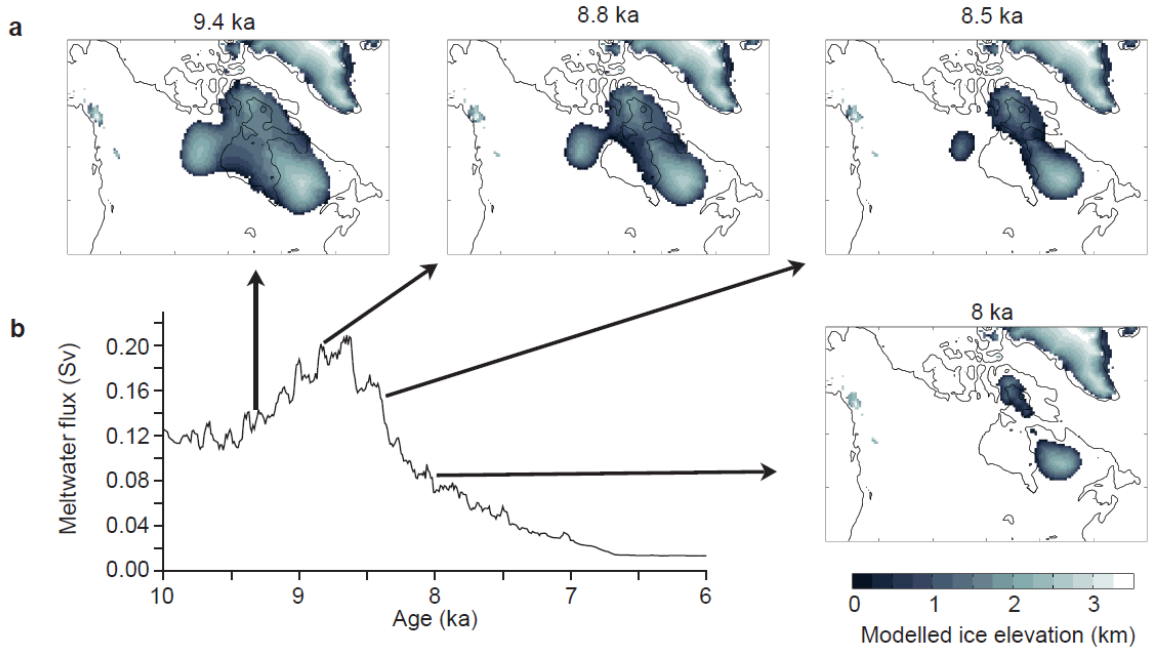

Figure 4: The 8,200 year event in our model. a, Evolution of ice sheet elevation and topography in North America before, during and at the end of the second meltwater pulse. **b,** Time series of the meltwater flux (in Sv) from the North American ice sheet between 10 ka and 6 ka. The ages correspond to model time.

Methods

Ice Sheet model description: The ice sheet model used in this study is Glimmer-CISM[14] version 1.0.14, a 3D-thermomechanical ice sheet model based on the shallow ice approximation. The model includes isostatic adjustment, basal sliding and a simple parameterisation for calving. It does not simulate ice shelves and does not include higher order physics, but thanks to its speed, it is well suited for simulating evolution of continental scale ice sheets over glacial-interglacial time-scales and is comparable to the models used to simulate Quaternary ice sheets[31–34].

Initial conditions: We started our simulation of the deglaciation with spun-up LGM North American ice sheet state, built-up through the last glacial-interglacial cycle using the standard snapshot interpolation technique[31–33]. This technique consists of interpolating present day and

Last Glacial Maximum (LGM ; 21 ka) equilibrium runs with a climate index proportional to the NGRIP $\delta^{18}O$ record[35]. This spinning-up of the ice sheet was initiated from the last interglacial period at 120 ka with present day topography and ice thickness[36]. We then used the LGM ice thickness, velocity, temperature and the bedrock topography obtained to initialise our deglaciation experiment.

Ice sheet model set-up: We use a horizontal resolution of 40 km, and 11 unequally spaced sigma levels to allow for higher resolution towards the bed of the ice sheet. When the basal conditions allow for melting, water accumulates, and the presence of basal water allows basal sliding to occur. To account for the presence of deformable sediment on the North American continent, which is likely to have been associated with high basal velocities, we prescribe a spatially varying basal sliding parameter. The basal sliding parameter is set to a high value B_{sed} where the sediment thickness[37] is greater than 20 m, otherwise it is set to a low value B_{rock}. We parameterised calving by cutting off floating ice. The isostatic adjustment of the bedrock to the ice load is calculated assuming the earth is composed of an elastic lithosphere (crust) floating on top of a relaxing mantle of time constant [38]. To calculate the mass balance, we used an annual Positive Degree Day (PDD) scheme[39]. This mass balance scheme works on the assumption that surface melting is proportional to the sum of positive degree days over a year. All precipitation is assumed to fall as snow, and up to 60 % of the snow fall can refreeze in the snow pack after melting. The parameter values we used for this study are presented in Table S1. Several parameter values were adjusted to improve the LGM ice volume, the LGM extent and the rate of uplift throughout the deglaciation compare to reconstructions[8]. These parameters are the relaxation time of the mantle, the basal sliding parameter and the flow factor of ice. We use a lapse rate of 5 °C km^{-1} [40]. A detailed comparison of our model results to observational data and ice sheet reconstruction and some sensitivity tests are described in Gregoire (2010)[30].

Climate forcing: To drive our ice sheet model through the last deglaciation, we used a transient climate model simulation performed with a low resolution ocean-atmosphere coupled GCM, called FAMOUS. This simulation was forced by boundary conditions varying through time with no acceleration factor. The boundary conditions changed through the climate simulation are the geography, trace gas concentrations, orbit and freshwater input (Figure S1). To account for changes in the sea level and ice sheets, the orography, bathymetry, land sea mask and ice sheet extent were updated every 1000 years according to the Ice-5G reconstruction[15]. The experiment is set up so that the ice sheet extent used between 21 ka and 20 ka is that of 21 ka, the ice extent used between 20 and 19 ka is that of 20 ka and so on. Except for area covered by ice, the vegetation is held constant at the present day values. Similarly, aerosols are held constant throughout the run. The atmospheric concentrations of CO_2, methane and N_2O are varied every time step with values taken from EPICA[41]. The simulation was forced with continuously varying insolation at the top of the atmosphere[42]. Finally freshwater is input into the ocean to reflect the discharge of ice sheets: this time varying field, based on a sea level reconstruction[43], consists of a background flux from the melting of the ice sheets and three meltwater pulses, Heinrich Event 1, MWP1a and Meltwater Pulse 1b (MWP1b). Heinrich Event 1 was put the Norwegian Sea and the Ice Rafter Debris (IRD) belt between 19 ka and 17 ka. For MWP1a, the equivalent of 15 m of sea level equivalent was released in the North Atlantic from 14.2 ka to 13.6 ka. MWP1b was mainly put into the Arctic Ocean releasing 5.6 m of sea level equivalent. No abrupt climate change was simulated over the deglaciation, in particular the Bølling-Allerød warming event and the Younger-Dryas cold periods are not reproduced in this simulation. The freshwater pulses input to the climate model had little impact on the climate. However, the climate simulation reproduces well the LGM and present day temperatures over Greenland and the overall rate of temperature change observed in Greenland ice cores. We forced the Glimmer

ice sheet model with monthly mean temperatures and precipitation. The temperatures are downscaled from the FAMOUS resolution, on a 7.5° longitude by 5° latitude grid, onto the Glimmer topography, on a 40 km grid, by using a constant lapse rate of 5 °C km^{-1}.

Smoothing of climate forcing: Because the climate model was run in 1,000-year intervals, ice sheet topography and extent in the climate model were changed abruptly at the start of each interval. This caused discontinuities in North American temperature and precipitation (Figure S2) that produced steps in the Glimmer ice sheet mass balance. We therefore transformed the output of the transient climate simulations to produce a smooth climate that we used to drive our ice sheet model (Figure S2). We first averaged the temperature and precipitation fields over 1,000 year intervals for each month of the year to produce long term mean climatologies. We then calculated the climate forcing by linearly interpolating between the 1,000-year climatological means for each month so that the changes in seasonal cycle are taken into account. This had the effect of removing artificial steps in the mass balance produced by the discontinuities in temperature and precipitation in the raw climate output.

Methods References

31. Marshall, S. J., James, T. S. & Clarke, G. K. C. North American Ice Sheet reconstructions at the Last Glacial Maximum. Quaternary Science Reviews 21, 175–192 (2002).

32. Charbit, S., Ritz, C., Philippon, G., Peyaud, V. & Kageyama, M. Numerical reconstructions of the Northern Hemisphere ice sheets through the last glacial-interglacial cycle. Clim. Past 3, 15–37 (2007).

33. Zweck, C. & Huybrechts, P. Modeling of the northern hemisphere ice sheets during the last glacial cycle and glaciological sensitivity. Journal of Geophysical Research-Atmospheres 110, 103–127 (2005).

382 34. Ganopolski, A., Calov, R. & Claussen, M. Simulation of the last glacial cycle with a
383 coupled climate ice-sheet model of intermediate complexity. Climate of the Past 6, 229–244
384 (2010).
385 35. NGRIP members High-resolution record of Northern Hemisphere climate extending into
386 the last interglacial period. Nature 431, 147–151 (2004).
387 36. Amante, C. & Eakins, B. W. ETOPO1 1 Arc-Minute Global Relief Model: Procedures,
388 Data Sources and Analysis. 19 (NOAA Technical Memorandum NESDIS NGDC: 2009).
389 37. Laske, G. & Masters, G. A global Digital Map of Sediment Thickness. EOS Trans. AGU
390 78, (1997).
391 38. Le Meur, E. & Huybrechts, P. A comparison of different ways of dealing with isostasy:
392 examples from modelling the Antarctic ice sheet during the last glacial cycle. Annals of
393 Glaciology 23, 309–317 (1996).
394 39. Reeh, N. Parameterization of Melt Rate and Surface Temperature in the Greenland Ice
395 Sheet. POLARFORSCHUNG 59, 113–128 (1991).
396 40. Abe-Ouchi, A., Segawa, T. & Saito, F. Climatic Conditions for modelling the Northern
397 Hemisphere ice sheets throughout the ice age cycle. Climate of the Past 3, 423–438 (2007).
398 41. Spahni, R. et al. Atmospheric Methane and Nitrous Oxide of the Late Pleistocene from
399 Antarctic Ice Cores. Science 310, 1317–1321 (2005).
400 42. Berger, A. & Loutre, M. F. Astronomical solutions for paleoclimate studies over the last 3
401 million years. Earth and Planetary Science Letters 111, 369–382 (1992).
402 43. Peltier, W. R. & Fairbanks, R. G. Global glacial ice volume and Last Glacial Maximum
403 duration from an extended Barbados sea level record. Quaternary Science Reviews 25, 3322–
404 3337 (2006).
405